Original Research Article: full paper

(2023), «EUREKA: Physics and Engineering»
Number 1

ANALYSIS OF FLOW CHARACTERISTICS OF CYLINDRICAL AND HELICAL TYPE MULTI-LOBE ROOTS BLOWER

Ngoc-Tien Tran✉
Department of Mechatronics Engineering[1]
tientn@haui.edu.vn

Duc-Minh Nguyen
Department of Mechatronics Engineering[1]

[1]*Hanoi University of Industry*
298 Cau Dien str., Bac Tu Liem District, Hanoi, Vietnam, 100000

✉**Corresponding author**

Abstract

Roots blower is a positive displacement machine that has the advantage of a larger flow than conventional blowers. Roots blowers are widely used in industrial production such as chemicals, food, medical, etc. However, during actual operation, this type of machine often achieves low performance. One of the issues that greatly affect performance is the flow characteristics of the blower. Flow characteristics include factors related to flow rate, pressure, and flow phenomena in the blower chamber. Flow characteristic analysis is a complex problem in hydraulic machines. Flow analysis helps to investigate the motion of the flow to design high-performance machines. This study uses a mathematical model of gear theory to design the rotor profile with cylindrical and helical lobes of the multi-lobe Roots blower. The rotor profile is formed on the principle that the ellipse rolls without slipping on the base circle. On the basis of the mathematical model of the rotor profile, the paper compares the flow rate and pressure characteristics of the two blowers. The fluid dynamics analysis model was built on ANSYS software. The structural grid model is also built to increase the computational efficiency of the mathematical model. The lobes are embedded and rotated in the blower chamber. The results show that with the same radial and axial dimensions, the cylindrical lobe has a larger flow. However, the helical lobe has a more stable flow quality than the cylindrical lobe (15.2 % less flow fluctuation). In terms of pressure, the helical lobe type has a higher pressure than the cylindrical lobe type. In addition, the helical lobe type also reduces the influence of eddy currents acting on the blower chamber walls and rotors. That results in increased blower efficiency. The results of the paper will be a reliable basis for reducing time in the development of multi-lobe Roots blowers with high performance.

Keywords: Roots blower, cylindrical lobe, helical lobe, CFD technique, ANSYS CFX.

DOI: 10.21303/2461-4262.2023.002578

1. Introduction

The Roots blower was invented by the Roots brothers in the 1860s [1]. Since then, Roots blower has been widely applied in various industries such as petroleum, chemical, and cement. The blower is also used as an air compressor in compressed air equipment or as a high-pressure blower with the advantage of large flow [2]. Scientists have been constantly working to improve the performance of the blower. One of the current prominent research directions is improving the rotor profile to increase the volume of air ejected after each rotation of the blower. A new rotor profile has been proposed by adding a scaling factor on the rolling circle to increase blower efficiency [3]. Three-lobe Roots blower has been proposed with the dedendum profile being a circular arc, the addendum profile having a partial arc, and an epicycloid [4, 5]. In [6], a new method of designing Roots blower rotors has been present by using the matching principle of non-circular gears and adjusting the design parameters according to a given flow rate. In [7], the authors improved the profile in [8] by using conjugate curves. In [9], two methods have been used that are DPD (Direct-Profile-Design) and DF (Deviation-Function) combined with the centrode curve design method in non-circular gears to change design parameters to create a new rotor profile. In [10], a new profile has been proposed by replacing the rolling circle with a rolling ellipse according to the formation principle of the epicycloid. The advantage of this design is that it is possible to change the semi-axes of the

ellipse to increase the volume of the blower cavity. This design is also the object of research that the authors present in this paper.

Recently, the CFD technique has shown to be effective and highly accurate in analyzing the flow dynamics of positive displacement machines. Therefore, there have been many studies analyzing the complex flow phenomena inside Roots blowers using the CFD technique. The clearances between the rotors were analyzed to improve the flow quality of the machine [11]. A new 3-D mesh model is developed for screw compressors [12]. The effect of compression on the deformation of the screw compressor has been determined [13]. The effect of clearance on flow oscillation of the blower using the RNG K-epsilon turbulence equation has been presented [14]. In [15], the authors compared turbulence models based on different mesh sizes to determine the efficiency of screw compressors. Kovacevic [16] used numerical CFD to investigate the pressure and velocity distribution across the cross-section of the screw compressors. The effects of pressure angles on the lobe pump have been analyzed in [17]. The flow is modeled in a three-lobed blower [18]. In this study, the authors used the K-epsilon turbulence model to determine the eddy current positions according to the change of the drive shaft rotation angle. K-epsilon (k–ε) turbulence model equations on SC/Tetra software to analyze flow characteristics and temperature changes during the machine's operation. Numerical simulation data are used to adjust the initial geometry to improve the aerodynamic efficiency of the blower [19]. In another study, the fictitious domain method to improve flow quality in a three-lobe rotor compressor has been applied [20]. In [21] these authors also continue to propose solutions to increase the meshing quality to improve the accuracy of the calculation results following the research presented in [19]. A solution to design the spiral outlet has been proposed to reduce pulse pressure and use numerical simulation to adjust the blower design [22].

In this study, let's use the rotor profile proposed by [10]. Let's design cylindrical lobe rotors and helical lobes. Finally, let's analyze the flow characteristics in the pumps by using the immersed method and the K-epsilon (k–ε) turbulence model.

2. Materials and methods

2. 1. Mathematical model of rotor addendum

As **Fig. 1** shows, the two mating rotors rotate in opposite directions on two parallel shafts.

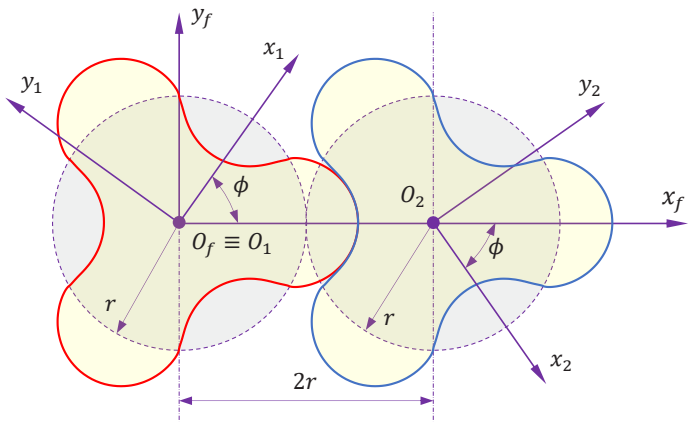

Fig. 1. The principle of designing the rotor profile

The coordinates systems $S_1(O_1x_1y_1)$, $S_2(O_2x_2y_2)$, and $S_f(O_fx_fy_f)$ are rigidly attached to the rotational axes of rotor 1, rotor 2, and the frame, respectively. According to [10], the addendum is formed on the basis of the locus of a fixed point on the ellipse when the ellipse rolls outside the base circle. The rotor addendum equation expressed in the coordinate system $S_1(O_1x_1y_1)$ is given by:

$$\mathbf{r}_1^{(S_1)} = \begin{bmatrix} x_1 \\ y_1 \\ 1 \end{bmatrix} = \begin{bmatrix} a\cos(\xi+\theta)(\cos\psi-1)+b\sin(\xi+\theta)\sin\psi+r\cos\theta \\ a\sin(\xi+\theta)(\cos\psi-1)-b\cos(\xi+\theta)\sin\psi+r\sin\theta \\ 1 \end{bmatrix}, \quad (1)$$

where a, b, r are semi-major axis, semi-minor axis of the ellipse and radius of the base circle, respectively. The angular parameters of (1) are given by:

$$\begin{cases} \xi = \tan^{-1}\dfrac{\partial_\psi x(\psi)}{\partial_\psi y(\psi)}, \\ \theta = \dfrac{1}{r_b}\int_0^\psi \left(\partial_\psi^2 x(\psi) + \partial_\psi^2 y(\psi)\right)^{\frac{1}{2}} \mathrm{d}\psi, \\ \begin{bmatrix} x(\psi) \\ y(\psi) \end{bmatrix} = \begin{bmatrix} -a\cos\psi \\ b\sin\psi \end{bmatrix}. \end{cases} \tag{2}$$

2. 2. Mathematical model of rotor dedendum

Mathematically, the dedendum rotor is the envelope to a family of addendum curves. The dedendum rotor equation $\mathbf{r}_2^{(S_2)}$ is determined via coordinate transformation:

$$\mathbf{r}_2^{(S_2)} = \mathbf{M}_{21}\mathbf{r}_1^{(S_1)}, \tag{3}$$

where

$$\mathbf{M}_{21} = \begin{bmatrix} \cos 2\phi & \sin 2\phi & -2r\cos 2\phi \\ -\sin 2\phi & \cos 2\phi & 2r\sin 2\phi \\ 0 & 0 & 1 \end{bmatrix}.$$

From equation (3) there is:

$$\mathbf{r}_2^{(S_2)} = \begin{bmatrix} x_2 \\ y_2 \\ 1 \end{bmatrix} = \begin{bmatrix} a(\cos\psi - 1)\cos(\xi + \theta - 2\phi) + b\sin\psi\sin(\xi + \theta - 2\phi) + r\left(\cos(\theta - 2\phi) - 2\cos\phi\right) \\ a(\cos\psi - 1)\sin(\xi + \theta - 2\phi) + b\sin\psi\cos(\xi + \theta - 2\phi) + r\left(\sin(\theta - 2\phi) + 2\cos\phi\right) \\ 1 \end{bmatrix}. \tag{4}$$

According to [10], (4) determine the relationship between the rotor angle parameter (ϕ) and the angle parameter of the ellipse (θ). Let's use the meshing equation:

$$\mathbf{N}_1 \cdot \mathbf{V}_1^{(S_1,S_2)} = 0, \tag{5}$$

where $\mathbf{N}_1$ is the normal vector given by:

$$\mathbf{N}_1 = \partial_\psi \mathbf{r}_1^{(S_1)} \times \mathbf{k} = \left(\partial_\psi x_1 \mathbf{i} + \partial_\psi y_1 \mathbf{j}\right) \times \mathbf{k} = N_{x1}(\psi)\mathbf{i} + N_{y1}(\psi)\mathbf{j}. \tag{6}$$

Relative velocity $\mathbf{V}_1^{(S_1,S_2)}$ is determined by:

$$\mathbf{V}_1^{(S_1,S_2)} = V_{x1}(\phi,\psi)\mathbf{i} + V_{y1}(\phi,\psi)\mathbf{j} = \left(-2r\sin\phi + 2y_1\right)\mathbf{i} + \left(-2x_1 + 2r\cos\phi\right)\mathbf{j}. \tag{7}$$

Replace equation (6) and equation (7) into equation (5), let's obtain:

$$f = \left(-2r\sin\phi + 2y_1\right)N_{x1}(\psi) + \left(-2x_1 + 2r\cos\phi\right)N_{y1}(\psi) = 0. \tag{8}$$

3. Results and discussion

3. 1. Governing equations

This study used the computational fluid dynamics on the CFX module of ANSYS software. The mathematical model is applied to the flow with a mathematical basis based on the governing equations. The continuity equation for fluid flow is given by:

$$\frac{\partial \mathbf{V}}{\partial t} + \nabla \cdot \rho \mathbf{V} = 0. \tag{9}$$

The equation of momentum in the form:

$$\rho\left[\frac{\partial \mathbf{V}}{\partial t}+(\nabla\cdot\mathbf{V})\mathbf{V}\right]\nabla p+(\nabla\tilde{\tau})=\rho\tilde{g}+f, \tag{10}$$

where p is the static pressure, $\tilde{\tau}$ is the stress tensor, $\rho\tilde{g}$ and **f** are the gravitational body force and surface forces, respectively. The turbulence of the fluid flow is determined via the equation k–ε:

$$\frac{\partial}{\partial t}(\rho k)+\nabla\cdot(\rho k V)=\nabla\cdot\left[\left(\mu+\frac{\mu_t}{\sigma_k}\right)\nabla k\right]+G_k+G_b-\rho\varepsilon-y_m+S_k, \tag{11}$$

$$\frac{\partial}{\partial t}(\rho\varepsilon)+\nabla\cdot(\rho\varepsilon V)=\nabla\cdot\left[\left(\mu+\frac{\mu_t}{\sigma_\varepsilon}\right)\nabla\varepsilon\right]+C_{1\varepsilon}\frac{\varepsilon}{k}(G_k+C_{3\varepsilon}G_b)-C_{2\varepsilon}\frac{\varepsilon^2}{k}+S_\varepsilon, \tag{12}$$

where the turbulent viscosity, $\mu_t=\rho C_\mu k^2/\varepsilon$ and the model constants: $C_{1\varepsilon}=1.44$, $C_{2\varepsilon}=1.92$, $C_\mu=0.09$, $\sigma_k=0.3$, $\sigma_\varepsilon=1.3$.

3. 2. Roots blower 3-D model

In this study, the three-lobe roots blower model was built based on the theory presented in section 2 with design parameters: $a=22.8563$ mm, $b=13.8563$ mm, $r=74.2874$ mm, rotor thickness $D=80$ mm, clearance between rotors $\Delta=0.01$ mm. The rotor profile is designed in CAD software, then Solidworks software is used to create the 3-D geometry of the cylindrical lobe and the helical lobe. The left rotor rotates clockwise and the right rotor rotates counterclockwise. The helical rotors are designed with a fixed angle of twist ($\beta=15$ deg). The CFD simulation model has two rotors immersed and rotated in the respective stator. The 3-D models are shown in **Fig. 2.**

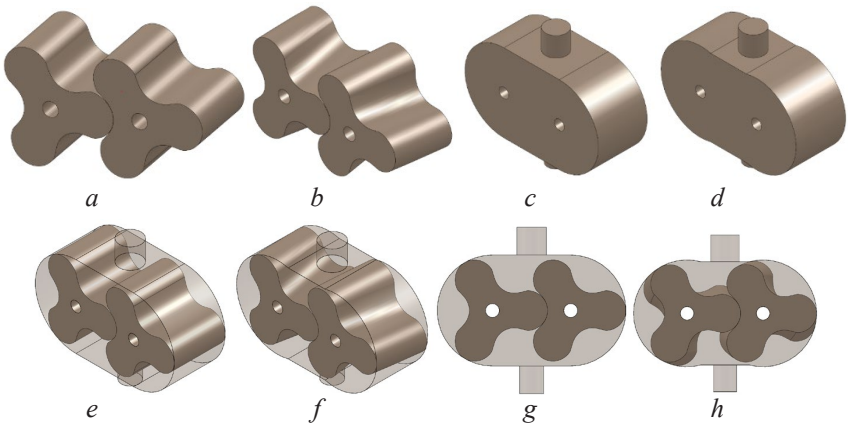

Fig. 2. Building 3-D models of cylindrical rotors and helical rotors:
a − cylindrical rotors model; *b* − helical rotors model; *c* − cylindrical stator model;
d − helical stator model; *e* − immersed cylindrical rotors model; *f* − immersed helical rotors model; *g* − immersed helical rotors model: front view;
h − immersed helical rotors model: front view

3. 3. Simulation parameters

This study builds simulation parameters for two types of blowers by using the CFX module of ANSYS software. Simulation parameters of the two types of blowers are the same for efficient and accurate investigation. Meshing parameters given in **Table 1** and **Fig. 3** corresponds to 2 types of cylindrical and helical rotors.

The numerical simulation model is determined in 4 working cycles of the blower. The rotation speed of the rotors is 1500 rpm. The physical characteristics of the mathematical model are given in **Table 2**.

Table 1
Simulation mesh parameters

Grid type	Rotor type	
	Cylindrical	Helical
Nodes	366622	346580
Elements	527302	508689
Max face size	7·e-003 m	7·e-003 m
Max Tet size	9·e-003 m	9·e-003 m

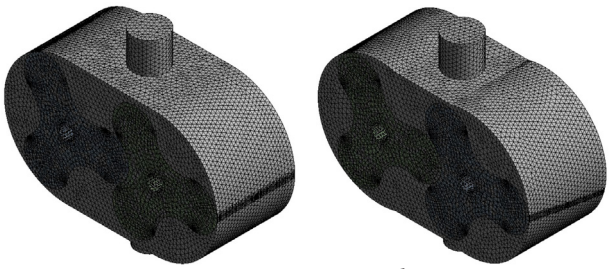

a *b*

Fig. 3. Grid structure of the model: *a* − grid structure of cylindrical lobe blower; *b* − grid structure of helical lobe blower

Table 2
Physical characteristics of the flow

Physical properties	Fluid type
Material	Air Ideal Gas
Domain type	Fluid Domain
Morphology	Continuous Fluid
Reference Pressure	1 bar
Heat Transfer	Isothermal
Fluid Temperature	25 [°C]
Velocity Type	Cartesian
Cartesian Velocity Components	Automatic with Value
U	0 [m·s^{-1}]
V	0 [m·s^{-1}]
W	0 [m·s^{-1}]
Turbulence	Medium (intensity = 5 %)

Flow rate and pressure are two characteristic parameters of the fluid flow in the blowers. The numerical simulation results of the two types of blowers are described in the graphs below. **Fig. 4, *a*, *b*** describe the instantaneous flow rate; **Fig. 4, *c*, *d*** describe the pressure at the outlet.

In this study, the effects of temperature and fluid loss through clearances during blower operation were not considered. From **Fig. 4** it is possible to see that: with the same axial and glass size, the flow value is similar in the two types of blowers (the percentage to represent the difference is about 0.89 %). However, the flow variation of the cylindrical lobe blower is 15.2 % larger than that of the helical type. It shows that the helical lobe has more flow stability than the cylindrical lobe. In terms of pressure, the helical lobe type has a higher pressure of 12.5 % than the cylindrical lobe type. **Fig. 5** shows the pressure distribution changes in the blower chamber of the cylindrical lobe and helical lobe during the blower operation. Rotation speed of rotors is constant at 1500 rpm. At the initial time, the pressure is equally distributed in the inlet chamber and outlet chamber. When the machine is running, the fluid will move due to the movement of the rotors. This movement is represented

by the pressure difference between the inlet and outlet of the blower. In addition, at the junction between the two rotors in the outlet chamber, the local pressure reaches the maximum value.

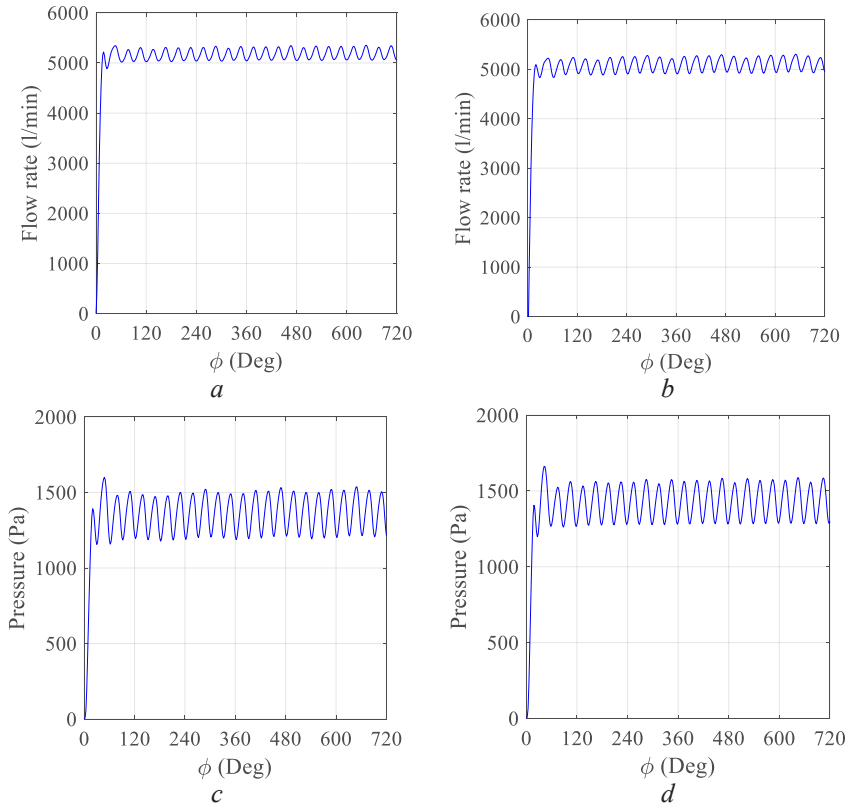

Fig. 4. Instantaneous flow rate and pressure of the blowers:
a − Instantaneous flow rate of cylindrical lobe blower; *b* − Instantaneous flow rate of helical lobe blower; *c* − Pressure of cylindrical lobe blower; *d* − Pressure of helical lobe blower

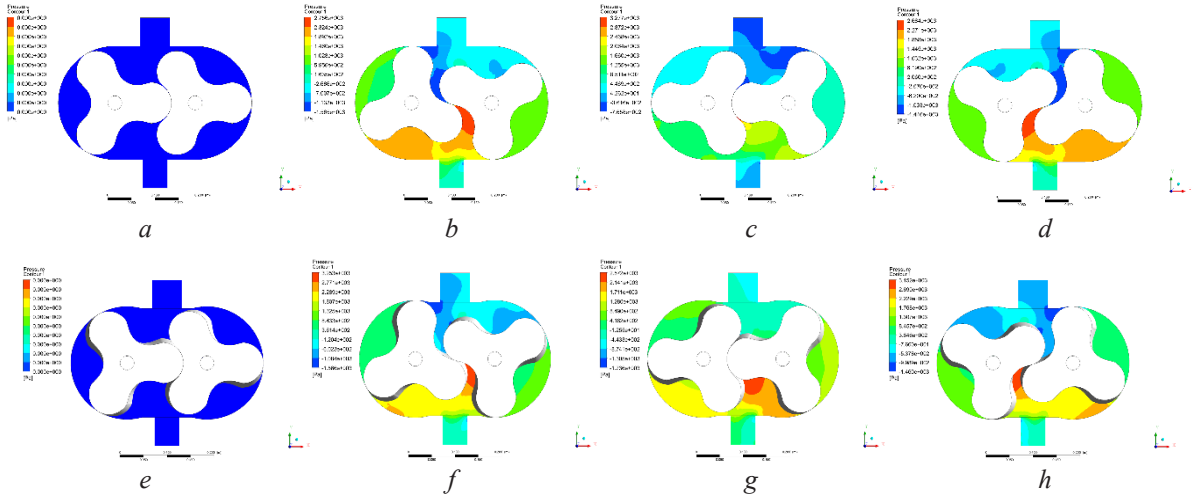

Fig. 5. Pressure distribution:
a − cylindrical lobe (ϕ = 0 deg); *b* − cylindrical lobe (ϕ = 45 deg);
c − cylindrical lobe (ϕ = 90 deg); *d* − cylindrical lobe (ϕ = 135 deg); *e* − Helical lobe (ϕ = 0 deg);
f − helical lobe (ϕ = 45 deg); *g* − helical lobe (ϕ = 90 deg); *h* − helical lobe (ϕ = 135 deg)

Fig. 6 shows the streamline in the blower chambers of the two types of blowers at different times. At the outlet of the helical blower, the streamline density of the flow is greater than

that of the cylindrical blower. In the helical blower chamber, the eddy current disappears and the stream flows smoothly, which means better flow quality than the cylindrical rotor.

Fig. 7 shows the variation of the velocity vector during the operation of the two types of the blowers. At the initial time, the variation of the velocity vector is zero in the two pump types. The speed of the velocity vector changes with each rotation of the rotor. This shows that the position of the lobes will affect the distribution of velocities in the pump chamber. On the other hand, the velocity at the outlet chamber also changes with the change of the drive shaft rotation angle. The velocity of the fluid in the inlet chamber is less than the velocity of the fluid in the outlet chamber. This change in flow velocity will affect the energy consumption significantly for the 2 types of blowers. Eddy currents corresponding to the impact of the fluid flow appear more for the cylindrical lobe blower. That shows that the energy loss of the cylindrical lobe will be more than that of the helical lobe. The paper's findings will be used to explore the flow characteristics of new high-efficiency machines in the future.

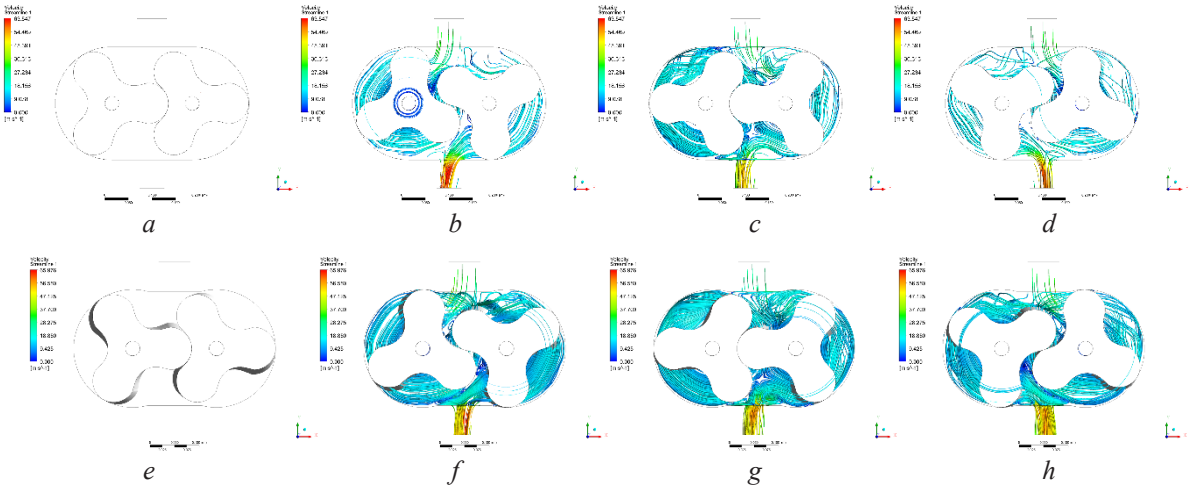

Fig. 6. Streamline distribution during blowers operation:
a − cylindrical lobe (ϕ = 0 deg); *b* − cylindrical lobe (ϕ = 45 deg); *c* − cylindrical lobe (ϕ = 90 deg);
d − cylindrical lobe (ϕ = 135 deg); *e* − helical lobe (ϕ = 0deg); *f* − helical lobe (ϕ = 45 deg);
g − helical lobe (ϕ = 90 deg); *h* − helical lobe (ϕ = 135 deg)

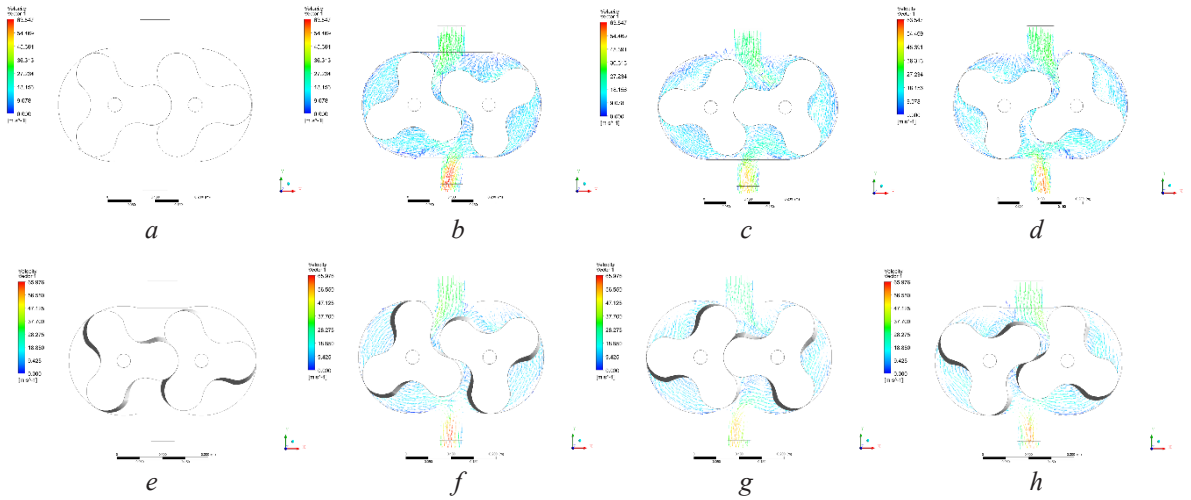

Fig. 7. Flow velocity vector during blowers operation:
a − cylindrical lobe (ϕ = 0 deg); *b* − cylindrical lobe (ϕ = 45 deg);
c − cylindrical lobe (ϕ = 90 deg); *d* − cylindrical lobe (ϕ = 135 deg); *e* − helical lobe (ϕ = 0 deg);
f − helical lobe (ϕ = 45 deg); *g* − helical lobe (ϕ = 90 deg); *h* − helical lobe (ϕ = 135 deg)

4. Conclusions

This study analyzes the flow characteristics of two types of roots blower with cylindrical lobes and helical lobes. The results presented in this study show that:

1) The flow rate of the cylindrical lobe is higher than that of the helical lobe, but this higher amount is not significant.

2) The flow oscillation of the helical lobe is 15.2 % less than that of the cylindrical lobe, demonstrating the helical lobe's flow stability.

3) Pressure analyses at blower inlet chambers show that the helical lobe has a 12.5 % greater pressure than the cylindrical lobe. The local pressure distribution in the blower chamber shows high-pressure positions during blower operation. Turbulent eddy currents are also less frequent in the helical lobe design.

4) The fluid dynamics analysis model shows the advantage of a helical lobe design when meeting the requirements of high pressure and flow stability. Thereby saving energy and improving the blower's performance.

5) The results of the paper are applied to investigate the flow characteristics of new high-efficiency machines in the future to satisfy the development of the blower.

Conflict of interest

The authors declare that they have no conflict of interest in relation to this research, whether financial, personal, authorship or otherwise, that could affect the research and its results presented in this paper.

Financing

The study was performed without financial support.

Data availability

Data will be made available on reasonable request.

References

[1] Roots, P. H., Roots, F. M. (1860). Pat. No. US 2369. Rotary blower.

[2] Tien, T. N., Thai, N. H. (2019). A novel design of the roots blower. Vietnam Journal of Science and Technology, 57 (2), 249. doi: https://doi.org/10.15625/2525-2518/57/2/13094

[3] Hsieh, C.-F., Hwang, Y.-W. (2008). Tooth profile of a Roots rotor with a variable trochoid ratio. Mathematical and Computer Modelling, 48 (1-2), 19–33. doi: https://doi.org/10.1016/j.mcm.2007.08.008

[4] Yao, L., Ye, Z., Dai, J. S., Cai, H. (2005). Geometric analysis and tooth profiling of a three-lobe helical rotor of the Roots blower. Journal of Materials Processing Technology, 170 (1-2), 259–267. doi: https://doi.org/10.1016/j.jmatprotec.2005.05.020

[5] Yao, L., Ye, Z., Cai, H., Dai, J. S. (2004). Design of a milling cutter for a novel three-lobe arc-cycloidal helical rotor. Proceedings of the Institution of Mechanical Engineers, Part C: Journal of Mechanical Engineering Science, 218 (10), 1233–1241. doi: https://doi.org/10.1243/0954406042369071

[6] Tong, S.-H., Yang, D. C. H. (2005). Rotor Profiles Synthesis for Lobe Pumps With Given Flow Rate Functions. Journal of Mechanical Design, 127 (2), 287–294. doi: https://doi.org/10.1115/1.1798271

[7] Kang, Y.-H., Vu, H.-H. (2014). A newly developed rotor profile for lobe pumps: Generation and numerical performance assessment. Journal of Mechanical Science and Technology, 28 (3), 915–926. doi: https://doi.org/10.1007/s12206-013-1159-7

[8] Litvin, F. L., Fuentes, A. (2004). Gear geometry and applied theory. Cambridge University Press. doi: https://doi.org/10.1017/cbo9780511547126

[9] Yang, D. C. H., Tong, S.-H., Lin, J. (1999). Deviation-Function Based Pitch Curve Modification for Conjugate Pair Design. Journal of Mechanical Design, 121 (4), 579–586. doi: https://doi.org/10.1115/1.2829502

[10] Hsieh, C.-F. (2015). A new curve for application to the rotor profile of rotary lobe pumps. Mechanism and Machine Theory, 87, 70–81. doi: https://doi.org/10.1016/j.mechmachtheory.2014.12.018

[11] Joshi, A. M., Blekhman, D. I., Felske, J. D., Lordi, J. A., Mollendorf, J. C. (2006). Clearance Analysis and Leakage Flow CFD Model of a Two-Lobe Multi-Recompression Heater. International Journal of Rotating Machinery, 2006, 1–10. doi: https://doi.org/10.1155/ijrm/2006/79084

[12] Arjeneh, M., Kovacevic, A., Rane, S., Manolis, M., Stosic, N. (2015). Numerical and Experimental Investigation of Pressure Losses at Suction of a Twin Screw Compressor. IOP Conference Series: Materials Science and Engineering, 90, 012006. doi: https://doi.org/10.1088/1757-899x/90/1/012006

[13] Stosic, N., Smith, I. K., Kovacevic, A. (2003). Opportunities for innovation with screw compressors. Proceedings of the Institution of Mechanical Engineers, Part E: Journal of Process Mechanical Engineering, 217 (3), 157–170. doi: https://doi.org/10.1177/095440890321700301

[14] Li, Y.-B., Guo, D.-S., Li, X.-B. (2018). Mitigation of radial exciting force of rotary lobe pump by gradually varied gap. Engineering Applications of Computational Fluid Mechanics, 12 (1), 711–723. doi: https://doi.org/10.1080/19942060.2018.1517053

[15] Kethidi, M., Kovacevic, A., Stosic, N., Smith, I. K. (2011). Evaluation of various turbulence models in predicting screw compressor flow processes by CFD. 7th International Conference on Compressors and Their Systems 2011, 347–357. doi: https://doi.org/10.1533/9780857095350.8.347

[16] Kovacevic, A., Stosic, N., Mujic, E., Smith, I. K. (2007). CFD Integrated Design of Screw Compressors. Engineering Applications of Computational Fluid Mechanics, 1 (2), 96–108. doi: https://doi.org/10.1080/19942060.2007.11015185

[17] Li, Y. B., Jia, K., Meng, Q. W., Shen, H., Sang, X. H. (2013). Flow simulation of the effects of pressure angle to lobe pump rotor meshing characteristics. IOP Conference Series: Materials Science and Engineering, 52 (3), 032022. doi: https://doi.org/10.1088/1757-899x/52/3/032022

[18] Huang, Z. F., Liu, Z. X. (2009). Numerical study of a positive displacement blower. Proceedings of the Institution of Mechanical Engineers, Part C: Journal of Mechanical Engineering Science, 223 (10), 2309–2316. doi: https://doi.org/10.1243/09544062jmes1503

[19] Liu, X., Lu, J. (2014). Unsteady flow simulations in a three-lobe positive displacement blower. Chinese Journal of Mechanical Engineering, 27 (3), 575–583. doi: https://doi.org/10.3901/cjme.2014.03.575

[20] Vande Voorde, J., Vierendeels, J., Dick, E. (2004). Flow simulations in rotary volumetric pumps and compressors with the fictitious domain method. Journal of Computational and Applied Mathematics, 168 (1-2), 491–499. doi: https://doi.org/10.1016/j.cam.2003.04.007

[21] Vande Voorde, J., Vierendeels, J., Dick, E. (2003). A force-based grid manipulator for ALE calculations in a lobe pump. Journal of Thermal Science, 12 (4), 318–322. doi: https://doi.org/10.1007/s11630-003-0037-5

[22] Liu, X., Lu, J., Gao, R., Xi, G. (2013). Numerical investigation of the aerodynamic performance affected by spiral inlet and outlet in a positive displacement blower. Chinese Journal of Mechanical Engineering, 26 (5), 957–966. doi: https://doi.org/10.3901/cjme.2013.05.957

Received date 15.09.2022
Accepted date 24.12.2022
Published date 19.01.2023

How to cite: *Tran, N.-T., Nguyen, D.-M. (2023). Analysis of flow characteristics of cylindrical and helical type multi-lobe roots blower. EUREKA: Physics and Engineering, 1, 67–75. doi: https://doi.org/10.21303/2461-4262.2023.002578*